Ultrahigh conversion efficiency of betavoltaic cell using diamond pn junction

T. Shimaoka, H. Umezawa, K. Ichikawa, J. Pernot, S. Koizumi

Applied Physics Letters ARTICLE scitation.org/journal/apl

Ultrahigh conversion efficiency of betavoltaic cell using diamond pn junction

Cite as: Appl. Phys. Lett. **117**, 103902 (2020); doi: 10.1063/5.0020135
Submitted: 28 June 2020 · Accepted: 30 August 2020 ·
Published Online: 11 September 2020

T. Shimaoka,[1,a),b)] H. Umezawa,[2,3] K. Ichikawa,[1] J. Pernot,[3] and S. Koizumi[1,a)]

AFFILIATIONS

[1]National Institute for Materials Science (NIMS), 1-1 Namiki, Tsukuba 305-0044, Japan
[2]National Institute of Advanced Industrial Science and Technology (AIST), 1-8-31 Midorigaoka, Ikeda, Osaka 563-8577, Japan
[3]University Grenoble Alpes, CNRS, Institut Néel, 38000 Grenoble, France

Note: This paper is part of the Special Topic on Ultrawide Bandgap Semiconductors.
[a)]**Authors to whom correspondence should be addressed:** SHIMAOKA.Takehiro@nims.go.jp and koizumi.satoshi@nims.go.jp
[b)]**Present address:** National Institute of Advanced Industrial Science and Technology (AIST), 1-8-31 Midorigaoka, Ikeda, Osaka 563-8577, Japan.

ABSTRACT

A betavoltaic cell, which directly converts beta particles into energy, is composed of a junction diode and a beta-emitting source. Because the cells can deliver electricity over a long operation life ranging from several years to a decade, they are promising devices for applications in remote locations such as outer space, deserts, and underground areas. Herein, we report efficient energy conversion using a diamond pn junction. We characterized the betavoltaic performance under electron-beam irradiation using scanning electron microscopy and observed an open-circuit voltage of 4.26 V, a fill factor of 0.85, and a semiconductor conversion efficiency of 28%. These are the best values reported thus far for betavoltaic cells. The efficiency is close to the theoretical Shockley–Queisser efficiency limit for betavoltaic cells.

Betavoltaic cells directly convert the energy of beta particles into electricity.[1] The operation principle of a betavoltaic cell is similar to that of a solar cell, except that the energy source is a beta-emitting isotope. In betavoltaic cells, semiconductor junctions play the role of energy conversion. These cells have the advantage of a long lifetime, which is determined by the half-life ($T_{1/2}$) of the beta-emitting radioisotopes. ^{3}H ($T_{1/2}=$ 12 yr) and ^{63}Ni ($T_{1/2}=$ 100 yr) are commonly used as beta sources.[2–4] Therefore, the cells can operate several decades to more than hundred years without external energy sources, such as sunlight, or charging. In addition, the specific energy of 3.3 Wh/Kg was reported using the diamond Schottky barrier diode (SBD) and ^{63}Ni, which is more than ten times higher than that of commercial fuel cells (0.1 Wh/Kg).[5] Betavoltaic cells are expected to be utilized for battery applications in remote locations such as outer space and underground areas.

An important performance parameter for betavoltaic cells is conversion efficiency. Olsen *et al.* theoretically estimated the conversion efficiency of betavoltaic cells using the Shockley–Queisser (SQ) model[6] modified for betavoltaics.[2] According to this model, the wide bandgap improves the conversion efficiency and open-circuit voltage.[4] A maximum conversion efficiency of approximately 30% can be reached on increasing the bandgap. From this perspective, wide-bandgap materials are advantageous for betavoltaic cells. Several studies on SiC and GaN betavoltaic cells have been conducted.[7–11] SiC betavoltaic cells show a high semiconductor conversion efficiency of 23%, which is more than twice that of Si betavoltaic cells.[8] Similarly, GaInP and AlInP have been studied as x-ray cells coupled with ^{55}Fe to reduce device damage through irradiation.[12,13] However, ultrawide-bandgap materials such as diamond, AlN, and BN can further improve the conversion efficiency.[4] Diamond betavoltaic cells using a Schottky junction have been studied.[5,14–16] Delfaure *et al.* reported a high semiconductor conversion efficiency of 11% in diamond Schottky barrier diode (SBD) betavoltaic cells.[14] Bormashov *et al.* reported diamond SBD betavoltaic modules with an output power on the order of nanowatts.[5] However, the conversion efficiency of diamond SBDs is far from the theoretical limit because the barrier height (∼2 V) of the SBD is less than half of the built-in potential of a diamond pn junction (∼4.5 V),[5] which is one of the highest built-in potentials of the semiconductor junction. Recent progress of the growth technique of the *n*-type diamond has enabled a diamond pn junction.[17] It has been studied in the field of ultraviolet light emission,[18] power electronics,[19] and radiation sensing.[20] Although there is a theoretical prediction of

the betavoltaic performance of the diamond pn junction,[4,21] there has been no experimental evaluation. In this study, we achieved the highest semiconductor conversion efficiency among the betavoltaic cells reported thus far by utilizing the large built-in potential of a diamond pn junction.[16] The conversion efficiency was close to that of the theoretical SQ limit.

We formed pseudo-vertical diamond pn diodes. Figure 1 shows the structure of the diamond pn diodes. Homoepitaxial p^+, p, n^-, and n^+ diamond layers were grown on a {111} high-pressure high-temperature (HPHT) type-Ib diamond substrate via microwave plasma-assisted chemical vapor deposition (MPCVD). The B- (p-type) and P-doped (n-type) diamond layers were grown using individual MPCVD systems. Figure 2 shows the impurity profiles of the sample measured through secondary-ion mass spectrometry. The thicknesses of the p^+, p, n^-, and n^+ layers were 2, 0.1, 1.8, and <0.1 μm, respectively. The impurity concentrations were [B]: 3×10^{19} cm^{-3} for the p^+ layer, [B]: 2×10^{18} cm^{-3} for the p layer, [P]: 1×10^{16} cm^{-3} for the n^- layer, and [P]: 1×10^{20} cm^{-3} for the n^+ layer. Highly P-doped diamond was grown using a homemade CVD reactor to enhance P incorporation into the diamond for reducing series resistance.[22] After the growth, mesa structures were formed by inductive coupling plasma etching with oxygen gas. Subsequently, Ohmic contacts were formed by the electron beam deposition of Ti/Mo/Au, both on the mesa structures of the n^+-layer and p^+-layers.[23] The diameters of the mesa structures and electrodes were 240 and 150 μm, respectively.

Then, we evaluated the power–voltage (P–V) and current–voltage (I–V) characteristics of the diodes under electron-beam irradiation. Figure 3 shows a schematic of the electron-beam irradiation and one-dimensional energy deposition profile of the electrons in the diamond. The profile was computed using the Monte Carlo simulation code CASINO.[24] For electron-beam irradiation, a scanning electron microscopy (SEM, FEI F80) system was used as the electron source. The measurement was performed at room temperature (300 K). The electron beam irradiation was performed under vacuum at 1.9×10^{-6} Torr. The energy loss between the e-Gun and the sample was negligible. The inset shows the top view of the mesa diode. Electron beams at the accelerating voltages of 5, 10, 15, and 20 kV were irradiated on top of the n^+ layer. The energy of the electron beam was close to the average energy of a typical beta source (e.g., ^{3}H: 5.7 keV and Ni: 17.4 keV). Here, the maximum penetration depths of the 5, 10, 15, and 20 keV

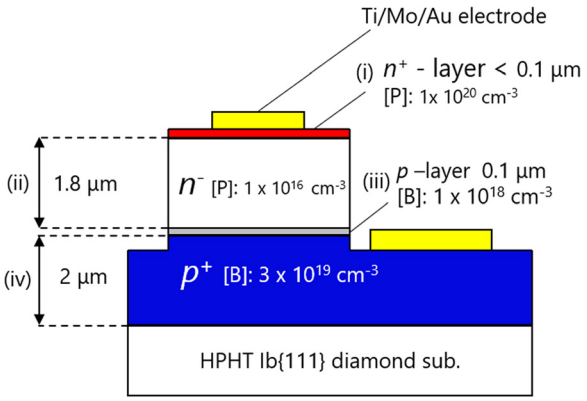

FIG. 1. Schematic of the diamond pn diode.

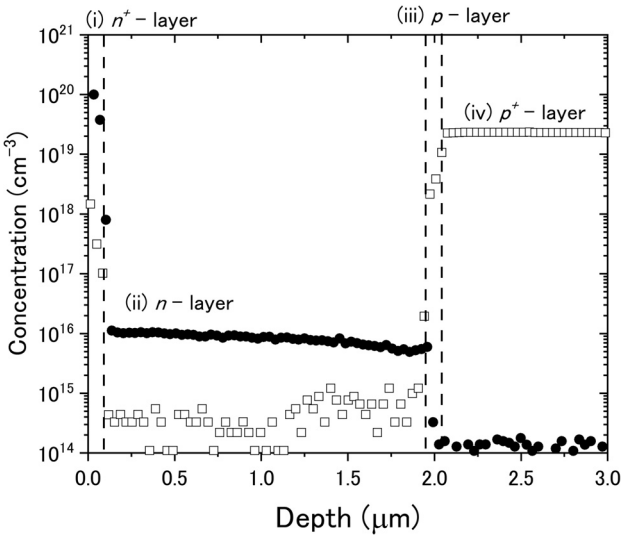

FIG. 2. Impurity depth profile of the diamond pn junction measured using secondary-ion mass spectrometry. The solid circles represent phosphorus and open squares represent boron.

electron beams estimated through the Monte Carlo simulation were 0.3, 0.8, 1.6, and 2.7 μm, respectively. We measured the dark current and current under electron-beam irradiation of the diode using a source meter (Keithley 2611B). The range of the voltage and the step of the sweep were −1 to 6 V and 50 mV, respectively. The beam current (I_{FC}) was measured using a Faraday cup to calibrate the current generated in the diodes. The uncertainty of the I_{FC} was within 0.3 pA. Under the electron beam irradiation, electron–hole pairs and excitons were created. The thermal equilibrium between excitons and free carriers was given as a function of a mass action law, exciton binding energy, and temperature.[25] At room temperature, we assumed the

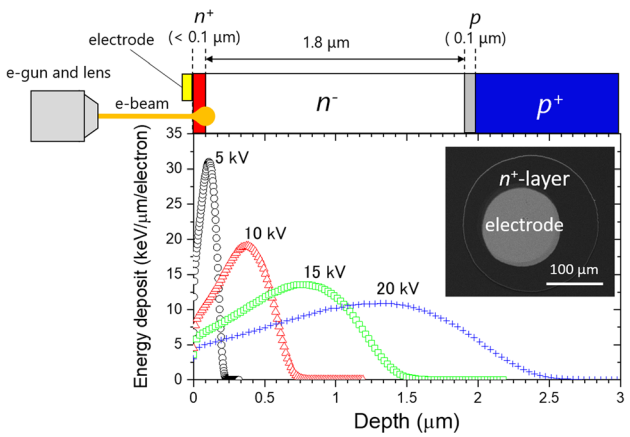

FIG. 3. Schematic of the electron-beam irradiation and one-dimensional energy deposition profile of electrons in diamond. Electron beams were irradiated on the top of the n^+ layer. The accelerating voltages were five (open circles), 10 (open triangles), 15 (open squares), and 20 kV (crosses). The inset shows the top view of the mesa diode.

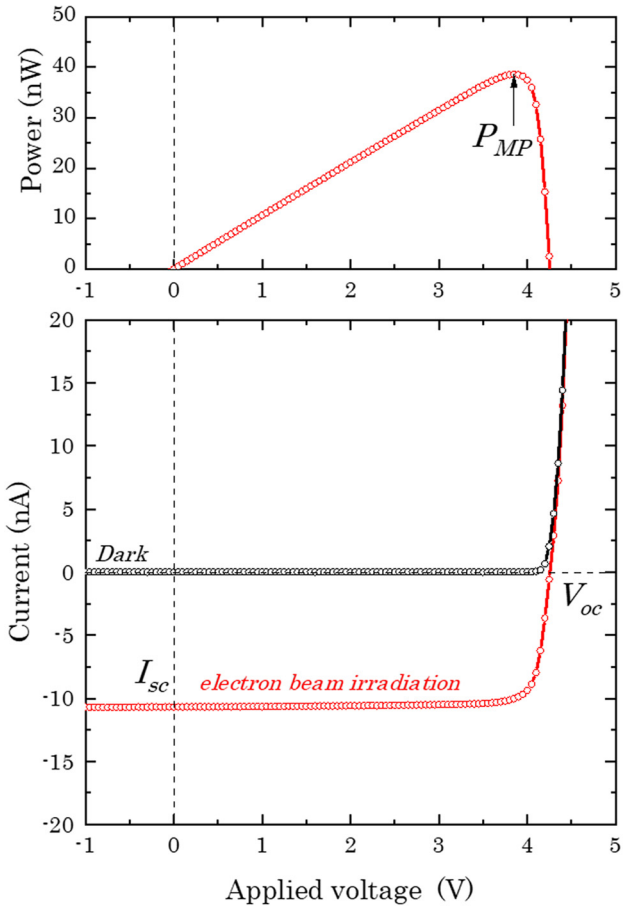

FIG. 4. *P–V* and *I–V* curves of the diamond pn diode at an accelerating voltage of 15 kV.

number of excitons created by electron-beam irradiation to be negligible compared with the number of electron–hole pairs.

Figure 4 shows the *P–V* and *I–V* characteristics of the pn diode under electron-beam irradiation with an accelerating voltage ($V_{acc.}$) of 15 kV. Table I summarizes the betavoltaic parameters including the open-circuit voltage (V_{oc}), short-circuit current (I_{sc}), output power at the maximum point (P_{MP}), and fill factor (*FF*) under electron-beam irradiation. V_{oc} was determined from the intersection of the *I–V* curve and x-axis. V_{oc} was 4.17–4.26 ± 0.03 V for $V_{acc.}$ = 5–20 kV, which is the highest observed in betavoltaic cells thus far. The *FF* was calculated as follows:[2,26]

$$FF = \frac{P_{MP}}{I_{SC} V_{OC}}. \tag{1}$$

The *FFs* were 0.774, 0.864, 0.848, and 0.824 ± 0.001 for $V_{acc.}$ = 5, 10, 15, and 20 kV, respectively. We also calculated the energy conversion efficiency η_s as follows:[2,26]

$$\frac{\eta_s}{100} = \frac{V_{OC} FF}{\epsilon}, \tag{2}$$

where ϵ is the electron–hole pair creation energy. Experimentally, the approximate ϵ value for charged particles is 12.8–13.6 eV.[5,27–29] In our work, we substituted ϵ = 13 eV in Eq. (2) and calculated the semiconductor conversion efficiency η_s, the values of which were 25%–28% for V_{acc} = 5–20 kV. The highest value was obtained for V_{acc} = 10 and 15 kV. Figure 5 compares the calculated η_s with the experimentally obtained efficiencies for Si,[30] GaAs,[31] SiC,[9] GaN,[11] and diamond. The dashed line in the figure represents the efficiency limit calculated by using the SQ model for betavoltaics.[2,4] Among the semiconductors, the diamond pn junction achieved the highest η_s, which is very close to the theoretical limit predicted by Olsen *et al.* In this approximation, the ϵ values of the materials were calculated using Klein's equation.[32] In reality, wide-bandgap materials have lower ϵ values than those determined using Klein's equation. By using the experimentally obtained ϵ value of diamond, the η_s of diamond can potentially reach ~35%.[21] To achieve this η_s value, V_{oc} should be further improved. V_{oc} is limited by the large ideality factor of the diamond pn junction ($n \sim 2$) owing to its high resistivity. We can further improve V_{oc} by forming n^+ diamond layers with low resistivity. If $V_{oc} > 4.5$ V, then η_s of the cell could exceed 30%.

Further, we calculated the total conversion efficiency η as follows:[2]

$$\eta = \eta_\beta \eta_c \eta_s, \tag{3}$$

where η_β and η_c denote the source efficiency and coupling efficiency, respectively. η_β is the fraction of electrons emitted from the source and directed to the device. η_c depends on the electron backscatter coefficient and collection efficiency of electron–hole pairs (Q) in the diode.

In this configuration, we set η_β as 100% because the electron beam was emitted from the electron gun of the SEM. η_c was determined as follows:

$$I_{EHP} = \frac{(1-r) I_{FC} V_{acc}}{\epsilon}, \tag{4}$$

$$Q = \frac{I_{sc}}{I_{EHP}}, \tag{5}$$

$$\eta_c = (1-r) Q, \tag{6}$$

TABLE I. Betavoltaic parameters of the diamond pn junction diode.

$V_{acc.}$ (kV)	V_{oc} (V)	I_{sc} (nA)	P_{MP} (nW)	*FF*	η_s (%)	I_{FC} (pA)	Q (%)	η_c (%)	η (%)
5	4.17 ± 0.03	0.42	1.36	0.774 ± 0.001	25	4.5 ± 0.3	25 ± 7	23 ± 6	5.8 ± 1.6
10	4.23 ± 0.03	3.78	13.8	0.864 ± 0.001	28	7.0 ± 0.3	73 ± 4	67 ± 4	19 ± 1
15	4.26 ± 0.03	10.7	38.6	0.848 ± 0.001	28	10.1 ± 0.3	95 ± 3	88 ± 3	24 ± 1
20	4.26 ± 0.03	18.1	63.5	0.824 ± 0.001	27	13.2 ± 0.3	93 ± 2	86 ± 2	23 ± 1

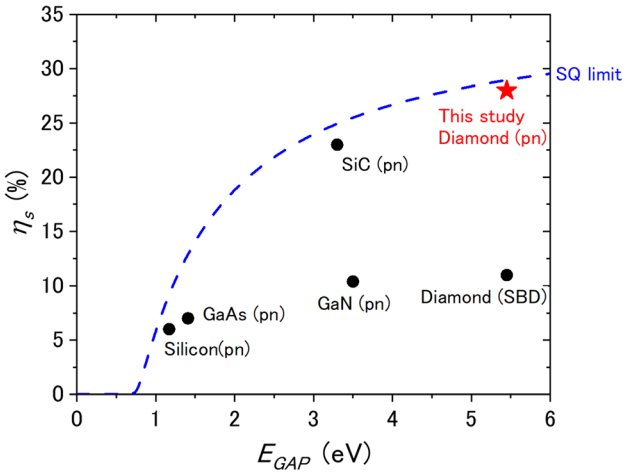

FIG. 5. Semiconductor conversion efficiency of the betavoltaic cells.[9,11,14,30,31] The dashed line represents the theoretical limit (Shockley–Queisser model),[2,4] the filled circles represent experimentally obtained values, and the filled star represents experimental data shown in this study.

where I_{EHP} represents the current resulting from the motion of electron–hole pairs created by the electron beam and r is the backscatter coefficient of electrons, which was estimated using the Monte Carlo simulation code CASINO.[24] These values are listed in Table I. The collection efficiency Q values estimated using Eqs. (5) and (6) were 25% ± 7%, 73% ± 4%, 95% ± 3%, and 93% ± 2% for V_{acc} = 5, 10, 15, and 20 kV, respectively. Furthermore, η_c values were 23% ± 6%, 67% ± 4%, 88% ± 3%, and 86% ± 2% for V_{acc} = 5, 10, 15, and 20 kV, respectively. The values of the total conversion efficiency η were 5.8% ± 1.6%, 19% ± 1%, 24% ± 1%, and 23% ± 1% for V_{acc} = 5, 10, 15, and 20 kV, respectively, under electron-beam irradiation. Because the highest Q value was obtained at V_{acc} = 15 kV, the loss in charge collection may be attributed to charge trapping or recombination in the highly doped n^+ and p^+ layers. As shown in Fig. 1, 5 keV and 20 keV electrons deposit approximately 40% and 10% of their energy in the n^+ or p^+ layer, respectively. The minority carrier diffusion length decreases when the doping concentration increases.[33]

To improve the total conversion efficiency, the doping profile and layer thickness must be optimally designed for the energy of electrons from beta sources. The thickness of the n^+ layer must be reduced to improve Q for low-energy electrons from ^{3}H ($E_{ave.}$ = 5.7 keV). A Q value of 95% for V_{acc} = 15 kV indicates that the diffusion length of the n^+ layer is approximately 20 μm (see the supplementary material for the estimation process). A high ratio between the layer thickness and diffusion length increases the Q value of the pn diode. Diamond grown via CVD could have higher purity than compound semiconductors because it is a single-element semiconductor. High-purity diamond layers could improve the diffusion length considerably, thus yielding a high Q value with a thickness of several tens of micrometers. This enables the diode to efficiently collect charge carriers generated by the maximum energy of the electrons from the beta source (e.g., ^{3}H: 18.6 keV and ^{63}Ni: 66.9 keV).

As diamond-based devices can operate at high temperatures with low leakage current because of their wide bandgap,[34] a diamond pn diode will be suitable for betavoltaic cells used in remote sensing applications under extreme conditions such as those during drilling for oil and gas and during space exploration using spacecraft. The realization of a diamond pn junction with a high open-circuit voltage and the best semiconductor conversion efficiency reported thus far is promising for the development of high-performance betavoltaic cells. To develop a practical betavoltaic device, the design of the cell, including the thickness of the beta source, structure of the device, and choice of the resistor and capacitor, is necessary to maximize the output power and storage efficiency.[5,35] In the future, we intend to fabricate diamond pn diodes with the area of ~mm^2 and evaluate the conversion efficiency coupled with a beta source.

See the supplementary material for the details of the estimation of the minority carrier diffusion length and simulation parameters for the Monte Carlo simulation code CASINO.

This study was partially supported by NEDO SIP (No. P14029), JSPS KAKENHI (Nos. 17K14914 and 18J01909), the JSPS Bilateral Joint Research Project (JPJSBP No. 120192917), and the JAEA Project on Wisdom Integration (No. 30I123), Japan. The authors would like to thank Dr. Fabrice Donatini of Institut Néel for the setup of SEM and EBIC measurement systems.

DATA AVAILABILITY

The data that support the findings of this study are available from the corresponding author upon reasonable request.

REFERENCES

[1]P. Rappaport, "The electron-voltaic effect in p−n junctions induced by beta-particle bombardment," Phys. Rev. **93**, 246 (1954).
[2]L. Olsen, "Review of betavoltaic energy conversion," in Proceedings of the 12th SPRAT (1993), pp. 256–267.
[3]M. G. Spencer and T. Alam, "High power direct energy conversion by nuclear batteries," Appl. Phys. Rev. **6**, 031305 (2019).
[4]S. Maximenko, J. Moore, C. Affouda, and P. Jenkins, "Optimal semiconductors for ^{3}H and ^{63}Ni betavoltaics," Sci. Rep. **9**, 10892 (2019).
[5]V. S. Bormashov, S. Y. Troschiev, S. A. Tarelkin, A. P. Volkov, D. V. Teteruk, A. V. Golovanov, M. S. Kuznetsov, N. V. Kornilov, S. A. Terentiev, and V. D. Blank, "High power density nuclear battery prototype based on diamond Schottky diodes," Diamond Relat. Mater. **84**, 41–47 (2018).
[6]W. Shockley and H. J. Queisser, "Detailed balance limit of efficiency of p-n junction solar cells," J. Appl. Phys. **32**, 510–519 (1961).
[7]C. J. Eiting, V. Krishnamoorthy, S. Rodgers, T. George, J. D. Robertson, and J. Brockman, "Demonstration of a radiation resistant, high efficiency SiC betavoltaic," Appl. Phys. Lett. **88**, 064101 (2006).
[8]M. V. S. Chandrashekhar, C. I. Thomas, H. Li, M. G. Spencer, and A. Lal, "Demonstration of a 4H-SiC betavoltaic cell," Appl. Phys. Lett. **88**, 033506 (2006).
[9]C. Thomas, S. Portnoff, and M. G. Spencer, "High efficiency 4H-SiC betavoltaic power sources using tritium radioisotopes," Appl. Phys. Lett. **108**, 013505 (2016).
[10]S. Tin and A. Lal, "Ultra-high efficiency power density thinned-down silicon carbide betavoltaics," in Proceedings of the PowerMEMS (2009), pp. 189–192.
[11]C. E. Munson, Q. Gaimard, K. Merghem, S. Sundaram, D. J. Rogers, J. de Sanoit, P. L. Voss, A. Ramdane, J. P. Salvestrini, and A. Ougazzaden, "Modeling, design, fabrication and experimentation of a GaN-based, ^{63}Ni betavoltaic battery," J. Phys. D **51**, 035101 (2018).
[12]S. Butera, M. D. C. Whitaker, A. B. Krysa, and A. M. Barnett, "Temperature effects on an InGaP (GaInP) ^{55}Fe x-ray photovoltaic cell," Sci. Rep. **7**, 4981 (2017).
[13]S. Butera, M. D. C. Whitaker, A. B. Krysa, and A. M. Barnett, "6 μm thick AlInP ^{55}Fe x-ray photovoltaic and ^{63}Ni betavoltaic cells," Semicond. Sci. Technol. **33**, 105003 (2018).

[14]C. Delfaure, M. Pomorski, J. de Sanoit, P. Bergonzo, and S. Saada, "Single crystal CVD diamond membranes for betavoltaic cells," Appl. Phys. Lett. **108**, 252105 (2016).
[15]V. Bormashov, S. Troschiev, A. Volkov, S. Tarelkin, E. Korostylev, A. Golovanov, M. Kuznetsov, D. Teteruk, N. Kornilov, S. Terentiev, S. Buga, and V. Blank, "Development of nuclear microbattery prototype based on Schottky barrier diamond diodes," Phys. Status Solidi **212**, 2539–2547 (2015).
[16]S. Tarelkin, V. Bormashov, E. Korostylev, S. Troschiev, D. Teteruk, A. Golovanov, A. Volkov, N. Kornilov, M. Kuznetsov, D. Prikhodko, and S. Buga, "Comparative study of different metals for Schottky barrier diamond betavoltaic power converter by EBIC technique," Phys. Status Solidi **213**, 2492 (2016).
[17]S. Koizumi, K. Watanabe, M. Hasegawa, and H. Kanda, "Ultraviolet emission from a diamond pn junction," Science **292**, 1899–1901 (2001).
[18]S. Koizumi, *Power Electronics Device Applications of Diamond Semiconductors* (Woodhead Publishing Ltd., San Diego, 2018).
[19]T. Makino, K. Yoshino, N. Sakai, K. Uchida, S. Koizumi, H. Kato, D. Takeuchi, M. Ogura, K. Ohyama, T. Matsumoto, H. Okushi, and S. Yamasaki, Appl. Phys. Lett. **99**, 061110 (2011).
[20]J. Holmes, J. Brown, F. A. Koech, H. Johnson, M. K. Benipal, P. Kandlakunta, A. Zaniewski, R. Alarcon, R. Cao, S. M. Goodnick, and R. J. Nemanich, "Performance of 5 μm PIN diamond diodes as thermal neutron detectors," Nucl. Instrum. Methods Phys. Res., Sect. A **961**, 163601 (2020).
[21]Y.-M. Liu, J.-B. Lu, X.-Y. Li, X. Xu, R. He, R.-Z. Zheng, and G.-D. Wei, "Theoretical prediction of diamond betavoltaic batteries performance using ^{63}Ni," Chin. Phys. Lett. **35**, 072301 (2018).
[22]R. Ohtani, T. Yamamoto, S. D. Janssens, S. Yamasaki, and S. Koizumi, "Large improvement of phosphorus incorporation efficiency in n-type chemical vapor deposition of diamond," Appl. Phys. Lett. **105**, 232106 (2014).
[23]T. Teraji, S. Koizumi, and H. Kanda, "Ohmic contacts for phosphorus-doped n-type diamond," Phys. Status Solidi A **181**, 129–139 (2000).
[24]D. Drouin, A. R. Couture, D. Joly, X. Tastet, V. Aimez, and R. Gauvin, "CASINO V2.42-A fast and easy to use modeling tool for scanning electron microscopy and microanalysis users," Scanning **29**, 92–101 (2007).
[25]J. S. Im, A. Moritz, F. Steuber, V. Harle, F. Scholz, and A. Hangleiter, "Radiative carrier lifetime, momentum matrix element, and hole effective mass in GaN," Appl. Phys. Lett. **70**, 631 (1997).
[26]M. A. Green, "General solar cell curve factor including the effects of ideality factor, temperature and series resistance," Solid State Electron. **20**, 265–266 (1977).
[27]S. F. Kozlov, R. Stuck, M. Hage-Ali, and P. Siffert, "Preparation and characteristics of natural diamond nuclear radiation detectors," IEEE Trans. Nucl. Sci. **22**, 160–170 (1975).
[28]C. Canali, E. Gatti, S. Kozlov, P. F. Manfredi, C. Manfredotti, F. Nava, and A. Quirini, "Electrical properties and performances of natural diamond nuclear radiation detectors," Nucl. Instrum. Methods **160**, 73–77 (1979).
[29]T. Shimaoka, J. H. Kaneko, Y. Sato, M. Tsubota, H. Shimmyo, A. Chayahara, H. Watanabe, H. Umezawa, and Y. Mokuno, "Fano factor evaluation of diamond detectors for alpha particles," Phys. Status Solidi **213**, 2629–2633 (2016).
[30]A. Krasnov, S. Legotin, K. Kuzmina, N. Ershova, and B. Rogozev, "A nuclear battery based on silicon p-i-n structures with electroplating ^{63}Ni layer," Nucl. Eng. Technol. **51**, 1978–1982 (2019).
[31]S. Butera, G. Lioliou, and A. M. Barnett, "Temperature effects on gallium arsenide ^{63}Ni betavoltaic cell," Appl. Radiat. Isot. **125**, 42–47 (2017).
[32]C. A. Klein, "Bandgap dependence and related features of radiation ionization energies in semiconductors," J. Appl. Phys. **39**, 2029–2038 (1968).
[33]K. Kumakura, T. Makimoto, N. Kobayashi, T. Hashizume, T. Fukui, and H. Hasegawa, "Minority carrier diffusion length in GaN: Dislocation density and doping concentration dependence," Appl. Phys. Lett. **86**, 052105 (2005).
[34]H. Umezawa, M. Nagase, Y. Kato, and S. Shikata, "High temperature application of diamond power device," Diamond Relat. Mater. **24**, 201–205 (2012).
[35]T. Kang, J. Kim, S. Park, K. Son, K. Park, J. Lee, S. Kang, and B. Choi, "Evaluation of a betavoltaic energy converter supporting scalable modular structure," ETRI J. **41**, 254 (2019).